Synchrotron Photoionization Study of the O(^{3}P) + Alpha-Angelica Lactone (AAL) at 550 and 700K

Golbon Rezaei and Giovanni Meloni*
Department of Chemistry, University of San Francisco, San Francisco, CA 94117 USA

Introduction

Accessible energy is crucial for the sustainability of modern societies.[1] During the last century, fossil fuels have been used as the main source of energy in the world.[2] Fossil fuel sources are diminishing while the global demand for energy is growing. Thus, investment in finding alternative fuels, which would be more efficient, sustainable, and environmentally friendly is increasing.[3-7] In recent years biofuels have been receiving great attention because of their potential in decreasing carbon emissions and providing a long-term renewable solution to unsustainable fossil fuels.[8,9]

Other advantages of biofuels to make them a more attractive alternative are their accessible source and their relative ease of processing.[10] Currently, lactones are some of the alternatives being produced.[11-13] Many lactones occur in a range of natural substances and they have many advantages over bioethanol.[14] One of the renewable lactonic biofuels that have attracted, which is one of the world's energy renewable source attention is alpha angelica lactone (AAL).

In this study, oxidation of AAL initiated by ground oxygen, O(^{3}P), was studied at 550 and 700 K using synchrotron radiation coupled with multiplexed photoionization mass spectrometry at the Lawrence Berkeley National Lab (LBNL). Photoionization spectra (PIS) and kinetic time traces were measured to identify primary products.

Methods

The experiment were performed at Chemical Dynamics Beamline 9.0.2 at the Advanced Light Source (ALS) of LBNL.[15] Reaction species were identified by multiplexed time and energy-resolved mass spectrometry coupled with tunable synchrotron radiation for photoionization. A three-dimensional data block, consisted of the ion signal as a function of photon energy (eV), mass-to-charge ratio (m/z), and reaction time (ms), was collected.[16] Two- dimensional slices of the three-dimensional data were obtained by fixing one variable ((Figure 1).

The reactants have negative signals from kinetic time curves (ion signal vs kinetic time) and products show positive signals. Figure 2 shows the kinetic time traces of primary products compared with the reactant which is multiplied by -1 at 550K. Then the signal was integrated in the 20-60 ms time range for minimizing the presence of nonprimary products at two temperatures.

In this research, the branching fraction of each primary product is calculated by the following equation:

$$Branching\ Fraction = \frac{C_P}{C_R} = \frac{S_P \sigma_R}{S_R \sigma_P} . \left(\frac{M_R}{M_P}\right)^{0.67}$$

P and R stand for the products and the reactant. C_P and C_R are concentrations of the product and reactant, S_P and S_R represent signals from the PIS at 11 eV in this study. M_P and M_R are the mass of primary products and reactant to the power of 0.67. $\boldsymbol{\sigma}_P$ and $\boldsymbol{\sigma}_R$ represent the energy-dependent PI cross-sections.

The structures of identified molecules were optimized by the CBS-QB3 composite method [17, 18] to find zero-point vibrational energy (E_0), which allows calculating the various thermodynamic quantities; for instance, enthalpy of reaction and adiabatic ionization energy (AIE). Then simulated PIS based on the Franck-Condon approximation were obtained using the B3LYP functional level of theory with the basis set of CBSB7.[19] The available literature or simulate PIS was used to identify the primary products (Figure 3).[20]

Results

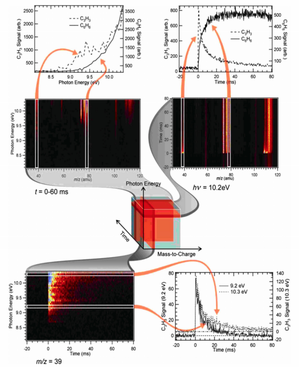

Figure1. Diagram of the three-dimensional dataset (the middle diagram) of photon energy, mass-to-charge ratio (m/z), and time (ms) obtained at the ALS in Berkeley, CA. PI curve (top left) and Time traces (top right). [16]

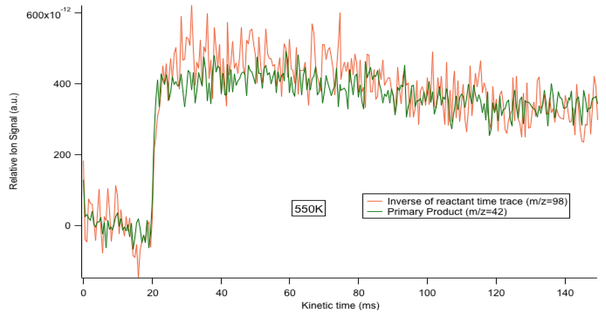

Figure 2. Kinetic time traces of primary product (m/z 42) and the inversed time traces of reactant at 550k. The kinetic time trace of the primary product matches well with the inverse curve of the reactant.

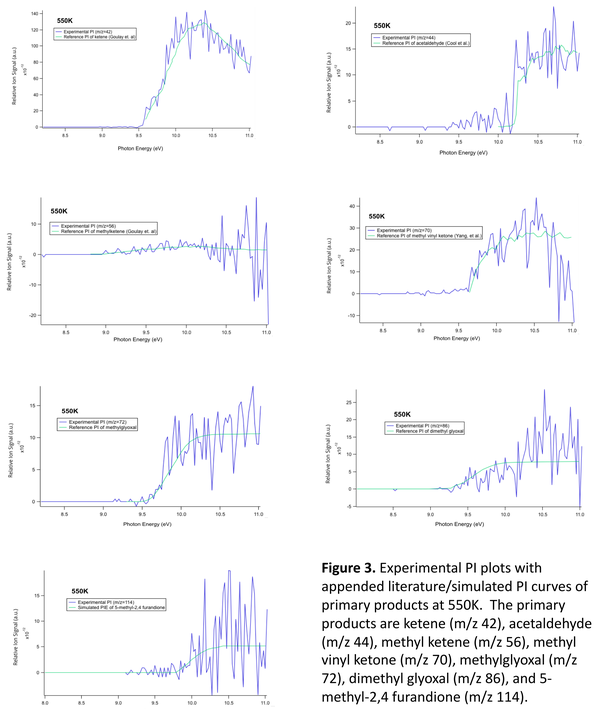

Figure 3. Experimental PI plots with appended literature/simulated PI curves of primary products at 550K. The primary products are ketene (m/z 42), acetaldehyde (m/z 44), methyl ketene (m/z 56), methyl vinyl ketone (m/z 70), methylglyoxal (m/z 72), dimethyl glyoxal (m/z 86), and 5-methyl-2,4 furandione (m/z 114).

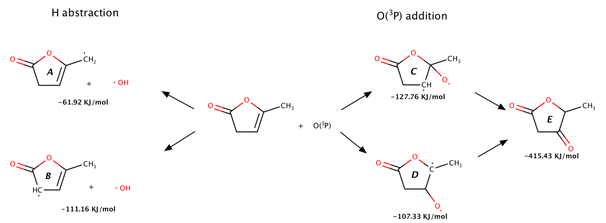

Scheme 1. Reaction pathways for H subtraction and for O(3P) addition. The energies that presented are relative to AAL and O(^{3}P).

Table 1. Primary products with mass-to-charge ratio and PI energy at 550K. The same products except for methyl ketene (m/z 56) and 5-methyl-2,4 furandione (m/z 114) are observed at 700 K.

Primary Product	Mass-to-charge ratio (m/z)	AIE (eV)
Ketene	42	9.58
Acetaldehyde	44	10.1
Methylketene	56	8.94
Methyl vinyl ketone	70	9.64
Methylglyoxal	72	9.59
Dimethyl glyoxal	86	9.11
5-methyl-2,4 furandione	114	9.83

Conclusions

In this experiment, two possible main reaction pathways are feasible, O(^{3}P) addition and hydrogen abstraction. The O(^{3}P) addition pathway is more favorable than hydrogen abstraction and it produces two triplet diradicals (C and D) which they end up with diketone (E). On the other hand, the hydrogen abstraction pathway forms the doublet radicals and O(^{3}P) binds to molecule A and B to generate products (scheme 1). The products of AAL and O(^{3}P) were identified by comparison with experimental PIS and literature or simulated PIS.

The primary products were identified based on their kinetic time traces. The observed primary products at 550 K are ketene (m/z 42), acetaldehyde (m/z 44), methyl ketene (m/z 56), methyl vinyl ketone (m/z 70), methylglyoxal (m/z 72), dimethyl glyoxal (m/z 86), and 5-methyl-2,4 furandione (m/z 114). The same products except for methyl ketene (m/z 56) and 5-methyl-2,4 furandione (m/z 114) are observed at 700 K.

Future Works

Ab initio calculations will be employed to study the potential energy surface to determine the reaction pathway leading to the formation of primary products. Also, branching fractions of primary products will be calculated.

Acknowledgments

This work is supported by the American Chemical Society– Petroleum Research Fund Grant # 56067-UR6. The authors also acknowledge Drs. Taatjes and Osborn from Sandia National Laboratories for the use of the experimental apparatus. The Advanced Light Source is supported by the Director, Office of Science, Office of Basic Energy Sciences, of the U.S. Department of Energy under Contract No.DEAC02-05CH11231.

References

1. Asif, M.; Muneer, T., Energy supply, its demand and security issues for developed and emerging economies. *Renew. Sust. Energ. Rev.* **2007**, *11*, 1388-1413.
2. Ranzan, L.; Ranzan, C.; Trierweiler, L. F.; Trierweiler, J. O. Classification of Diesel Fuel Using Two-Dimensional Fluorescence Spectroscopy. *Energy & Fuels* **2017**, *31* (9), 8942–8950.
3. Atsumi, S.; Hanai, T.; Liao, J. C. Non-Fermentative Pathways for Synthesis of Branched-Chain Higher Alcohols as Biofuels. *Nature* **2008**, *451* (7174), 86–89.
4. Hill, J.; Nelson, E.; Tilman, D.; Polasky, S.; Tiffany, D. Environmental, Economic, and Energetic Costs and Benefits of Biodiesel and Ethanol Biofuels. *Proceedings of the National Academy of Sciences* **2006**, *103* (30), 11206–11210.
5. Kohse-Höinghaus, K.; Oßwald, P.; Cool, T. A.; Kasper, T.; Hansen, N.; Qi, F.; Westbrook, C. K.; Westmoreland, P. R. Biofuel Combustion Chemistry: From Ethanol to Biodiesel. *Angewandte Chemie International Edition* **2010**, *49* (21), 3572–3597.
6. Vispute, T. P.; Huber, G. W. Breaking the Chemical and Engineering Barriers to Lignocellulosic Biofuels. *Int. Sugar J.* **2008**, *110*, 138–149.
7. Malpani, S.; Joseph, E. 2,5-Dimeethylfuran As A Bio-Fuel. *J. Environ. Sci., Toxicol. Food technol.* **2015**, 9(5), 71-72.
8. Kohse-Höinghaus, K.; Oßwald, P.; Cool, T. A.; Kasper, T.; Hansen, N.; Qi, F.; Westbrook, C. K.; Westmoreland, P. R. Biofuel Combustion Chemistry: From Ethanol to Biodiesel. *Angewandte Chemie International Edition* **2010**, *49* (21), 3572–3597.
9. Escobar, J. C.; Lora, E. S.; Venturini, O. J.; Yáñez, E. E.; Castillo, E. F.; Almazan, O. Biofuels: Environment, Technology and Food Security. *Renewable and Sustainable Energy Reviews* **2009**, *13* (6-7), 1275–1287.
10. Fathi, Y.; Meloni, G. Study of the Synchrotron Photoionization Oxidation of 2-Methylfuran Initiated by O(3P) under Low-Temperature Conditions at 550 and 650 K. *The Journal of Physical Chemistry A*, **2017**, *121* (37), 6966–6980.
11. Mehdi, H.; Fábos, V.; Tuba, R.; Bodor, A.; Mika, L. T.; Horváth, I. T. Integration of Homogeneous and Heterogeneous Catalytic Processes for a Multi-Step Conversion of Biomass: From Sucrose to Levulinic Acid, γ-Valerolactone, 1,4-Pentanediol, 2-Methyl-Tetrahydrofuran, and Alkanes. *Topics in Catalysis* **2008**, *48* (1-4), 49–54.
12. Horváth, I. T.; Mehdi, H.; Fábos, V.; Boda, L.; Mika, L. T. γ-Valerolactone—a Sustainable Liquid for Energy and Carbon-Based Chemicals. *Green Chem.* **2008**, *10* (2), 238–242.
13. Bond, J. Q.; Alonso, D. M.; Wang, D.; West, R. M.; Dumesic, J. A. Integrated Catalytic Conversion of -Valerolactone to Liquid Alkenes for Transportation Fuels. *Science* **2010**, *327* (5969), 1110–1114.
14. Cotton, S. Lactones as Biofuel.https://edu.rsc.org/soundbite/lactones-as-biofuel/2021245.article (accessed April 1, 2020).
15. Heimann, P. A.; Koike, M.; Hsu, C. W.; Blank, D.; Yang, X. M.; Suits, A. G.; Lee, Y. T.; Evans, M.; Ng, C. Y.; Flaim, C.; Padmore, H. A. Performance of the Vacuum Ultraviolet High-Resolution and High-Flux Beamline for Chemical Dynamics Studies at the Advanced Light Source. *Review of Scientific Instruments* **1997**, *68* (5), 1945–1951.
16. Osborn, D. L.; Zou, P.; Johnsen, H.; Hayden, C. C.; Taatjes, C. A.; Knyazev, V. D.; North, S. W.; Peterka, D. S.; Ahmed, M.; Leone, S. R. The Multiplexed Chemical Kinetic Photoionization Mass Spectrometer: A New Approach to Isomer-Resolved Chemical Kinetics. *Review of Scientific Instruments* **2008**, *79* (10), 104103.
17. Montgomery, J. A.; Frisch, M. J.; Ochterski, J. W.; Petersson, G. A. A Complete Basis Set Model Chemistry. VI. Use of Density Functional Geometries and Frequencies. *The Journal of Chemical Physics* **1999**, *110* (6), 2822–2827.
18. Montgomery, J. A.; Frisch, M. J.; Ochterski, J. W.; Petersson, G. A. A Complete Basis Set Model Chemistry. VII. Use of the Minimum Population Localization Method. *The Journal of Chemical Physics* **2000**, *112* (15), 6532–6542.
19. Baulch, D. L.; Bowman, C.T. Cobos, C.J.; Cox, R. A.; Just, T.; Kerr, J. A.; Pilling, M. J.; Stocker, D.; Troe, J.; Tsang, W.; Walker, R. W.; Warnatz, J., Evaluated kinetic data for combustion modeling: supplement II. *J. Phys. Chem. Ref. Data* **2005**, 34, 757-1397.
20. Fukui, K., Formulation of the Reaction Coordinate. *The Journal of Physical Chemistry.* **1970**, 74, 4161-4163.